Compressive behavior of wood I-joist under elevated temperature

Byrne T. Miyamoto†
Structural Testing Coordinator
TallWood Design Institute
Oregon State University, Corvallis, OR 97331
Email: byrne.miyamoto@oregonstate.edu

*Arijit Sinha**†
Professor and JELD-WEN Chair
Department of Wood Science and Engineering
Oregon State University, Corvallis, OR 97331
Email: Arijit.sinha@oregonstate.edu

(Received 12 June 2025)

Abstract. Wood composite I-joists are commonly used in residential construction and light commercial buildings, particularly in floor and roof assemblies. These assemblies are often fire-rated, based on building design, to meet specific safety standards. Fire-rated assemblies are constructed using manufacturer-specified materials such as gypsum board and fire-retardant plywood. While I-joists may not be directly exposed to flames, they can still experience significant thermal exposure. This study investigates the effects of elevated temperatures on the compressive strength and modulus of elasticity (MOE) of I-joists, with 90 specimens tested across various temperatures and two exposure durations. Results indicate that significant degradation in mechanical properties occurs around 190°C, with OSB web buckling identified as the primary failure mechanism. A Sigmoidal model was applied to capture the temperature-dependent degradation, revealing critical property decline near 200°C and higher. This research provides insights into the thermal behavior of I-joists, with implications for maintaining structural integrity in high-temperature environments, and highlights the need for further studies on long-term exposure and temperatures above 200°C.

Keywords: Wood composite I-joist; Compression strength; Elevated temperature

Introduction

Wood-composite I-joists, first developed in the 1960s, gained widespread adoption in construction during the late 1980s and 1990s due to their efficiency and improved performance over traditional solid wood joists (Fisette 2000). These joists are constructed from two primary components, the flanges, typically made from laminated veneer lumber (LVL), which form the top and bottom horizontal sections, and the web, often made from oriented strand board (OSB), which forms the vertical section (Smulski 1997). This "I" cross-sectional shape, similar to that of steel I-beams, provides excellent load-bearing capabilities, making I-joists ideal for residential and light commercial applications.

The transition to wood-composite I-joists has been driven largely by their cost-effectiveness and superior mechanical performance compared to solid wood joists. I-joists are manufactured from lower-cost tree species and smaller-diameter logs, reducing material costs while maintaining comparable strength to solid wood. In addition, their engineered design minimizes natural defects such as knots and splits, which are common in solid wood, resulting in more reliable structural performance (APA 2024a; Forest Products Laboratory 2010). Despite their increased popularity, some countries, including the United Kingdom and Canada, have implemented restrictions on I-joist usage due to concerns over fire performance. In the United States, certain jurisdictions have also considered limitations, though the National Association of Home Builders (NAHB) has actively opposed such restrictions in 1999 and again in 2023 (NAHB 1999, 2023).

An important mechanical advantage of I-joists is that they span longer distances than traditional joists, allowing for larger open spaces in architectural designs, a feature that is highly valued in modern construction (APA 2024a). Moreover, I-joists exhibit superior dimensional stability, meaning they

* Corresponding author
† Society of Wood Science & Technology member

Wood and Fiber Science, 57(4), 2025, pp. 178–186
https://doi.org/10.22382/wfs-2025-15

are less prone to shrinkage, swelling, warping, and cupping, enhancing their long-term structural reliability (Forest Products Laboratory 2010). This combination of mechanical strength, stability, and cost-efficiency makes I-joists a common solution in both residential and commercial construction, particularly in applications that demand both flexibility and durability.

In construction, I-joists are commonly used in floors, roofs, and ceiling systems, although they may occasionally serve as wall studs or beams. Fire performance of these systems depends on the assembly in which they are installed, as I-joists themselves are not fire-rated. A common testing standard used to determine fire performance of materials is ASTM E119 (ASTM International 2020), where assemblies are exposed to a time-temperature curve under constant load to simulate real-world conditions (Sultan et al. 2007; APA 2024b). Under this standard, unprotected I-joist assemblies can fail in less than 15 minutes under fire testing conditions (APA 2007). For this reason, in most building systems, the fire protection of I-joists follows the guidelines from the International Residential Code (IRC) which includes the use of gypsum drywall, mineral wool insulation, or fire-treated plywood (ICC 2024). Following these guidelines, in proper fire-rated assemblies, under ASTM E119, I-joists can achieve fire ratings of one hour or more.

In building assemblies, the primary stresses experienced by I-joists are flexural stresses. Most research on I-joists has focused on their flexural properties. Studies by King et al. (2014) and Way et al. (2018) have shown that environmental factors, such as moisture and weathering, can degrade the flexural performance of I-joists. Similarly, studies by Morrissey et al. (2009) and Yeh and Herzog (2018) have investigated the impact of holes drilled for utilities on the structural integrity of I-joists. Although I-joists are not typically subjected to significant compressive forces in standard applications, localized compression can occur in scenarios such as short spans or improperly reinforced openings. While the compressive properties of I-joist web stock have been studied (e.g., Grandmont et al. 2010), little research has focused on the compressive performance of I-joists under uniform loads, particularly at elevated temperatures. Localized compressive stresses exacerbate failure at elevated temperatures, as was evident in Sultan et al. (2007), and therefore, further investigation is needed.

In fire conditions, even if I-joists are not exposed to direct flames, assemblies can still reach elevated temperatures that degrade the LVL and OSB components. Degradation has been observed at temperatures starting around 150°C (Sinha et al. 2011; Forest Products Laboratory 2010). Despite this, the effects of elevated temperatures on the compressive properties of wood-composite I-joists remain understudied.

This study aims to evaluate the compressive properties of wood-composite I-joists at elevated temperatures by applying a uniform vertical load to 301 mm x 304 mm specimens. The testing was conducted at nine temperatures ranging from 120°C to 200°C, with two exposure times. The objectives of the study were to:

- Compare the effects of exposure times at elevated temperatures on the compressive strength and stiffness of wood-composite I-joists.
- Investigate the compressive properties of wood-composite I-joists at elevated temperatures.
- Model the relationship between elevated temperature, exposure time, and compressive performance using a Sigmoidal model.

Materials

The testing was conducted on wooden I-joists procured from a local manufacturer with a country-wide distribution chain. These were then cut to dimensions of 301.6 mm (~1 ft) in depth and 304 mm (1 ft) in length. The I-joists consisted of an 11-mm-thick web made of OSB, while the flanges were constructed from Douglas-fir laminated veneer lumber (LVL) with a depth of 30 mm and a width of 50.8 mm. This specific I-joist size was selected because it is commonly used in industry. The measured specific gravity of the OSB used in the I-joist web was 0.59. The specimen size was based on ASTM D7672-14 (ASTM International 2014), the Standard Specification for Evaluating Structural Capacities of Rim Board Products and Assemblies, which prescribes a minimum length of 304 mm for vertical load testing. A total of 90 I-joists pieces were tested across nine different temperatures and two exposure times, as outlined in Table 1. The I-joists were conditioned at 20°C and 65% relative humidity until the material reached an approximate equilibrium moisture content of 12% (±3%), as seen in Figure 1a.

Table 1. Testing matrix for I-joist.

Exposure	Testing temperatures (°C)									Total
	120	130	140	150	160	170	180	190	200	
0 min.	5	5	5	5	5	5	5	5	5	45
50 min.	5	5	5	5	5	5	5	5	5	45
Total	10	10	10	10	10	10	10	10	10	90

Figure 1. Samples and compression test setup. (A) I-Joist conditioned room; (B) Testing setup with BEMCO installed within INSTRON testing frame; (C) Typical specimen installation with tested specimen and heating specimen.

Methods

Testing was conducted in accordance with ASTM D7672 (ASTM International 2014) Standard for Evaluating Structural Capacities of Rim Board Products and Assemblies. The tests were performed under uniform vertical load conditions using an INSTRON 5546, equipped with a Bemco environmental chamber integrated into the testing frame. The chamber had two access points, one at the top and the other at the bottom, allowing extension arms fitted with compression platens to extend from both the INSTRON testing base and crosshead, as shown in Figure 1b. This configuration allowed testing at elevated temperatures within the chamber while preventing any direct force from being applied to the Bemco chamber itself.

Thermocouples were installed in both the flange and web of the I-joists to monitor temperature. Two specimens were placed in the chamber, one for testing and the other for pre-heating (as shown in Figure 1c). Once the target temperature was reached for the specimen to be tested, the test was conducted. Afterward, the failed specimen was replaced by the pre-heated one, and a new specimen was placed in the chamber to pre-heat. A slight temperature drop occurred during the transfer, so the specimens were reheated to ensure uniformity before testing. The flange required approximately 20–30 minutes to heat, while the web took 10–15 minutes. This timing allowed sufficient time for testing before the next specimen reached the target temperature. Testing commenced once both the flange and web achieved the target temperature.

Tests were performed at nine temperatures, ranging from 120°C to 200°C, with 10°C increments. Two testing durations were used: one immediately after the specimen reached the prescribed temperature, and the other after 50 minutes of exposure. Once the specimen reached the target temperature and time, it was preloaded to approximately 170 N and tested at a rate of 1.25 mm/min until failure. Force measurements were taken from a 300 kN load cell attached to the INSTRON crosshead, and deflection was measured via crosshead displacement.

Following testing, both the compressive strength and compressive modulus of elasticity (MOE) of the I-joist were calculated.

Compressive strength (σc) was determined using the following equation:

$$\sigma_c = \frac{F_{max}}{A} \quad [1]$$

Where, σ_c is the compressive strength in MPa, F_{max} was the maximum applied force, and A is the cross-sectional area of the OSB web.

The compressive modulus of elasticity (E) was calculated using the following equation:

$$E = \frac{\Delta F}{d * \Delta \delta} \quad [2]$$

Where, E is the modulus of elasticity of the I-joist, ΔF is the change in load (N) within the elastic region, Δδ is the change in deflection (mm) in the elastic region, and d is the thickness of the OSB web in mm. The elastic range used for ΔF and Δδ, was approximately 10%–40% of the maximum force.

Results and Discussion

The results for compressive strength and compressive MOE of the I-joists are presented in Table 2 and Table 3, respectively. Table 2 provides the average compressive strength at each tested temperature, while Table 3 displays the average MOE for each temperature. These results offer a detailed comparison of how temperature affects both the strength and stiffness properties of the I-joists.

When examining the influence of exposure time on both compressive strength and stiffness, the results suggest that exposure duration did not significantly degrade these properties over time. This conclusion is supported by T-tests conducted at each temperature to compare the two exposure durations. For compressive strength, no significant differences were observed between exposure times except at 140°C (p-value = 0.01). A similar pattern was found for MOE, with a statistically significant difference only at 160°C (p-value = 0.02). These p-values are reported in Tables 2 and 3.

The stability of mechanical properties under elevated temperatures is likely due to the heat-resistant adhesive used in the I-joists, which meets ASTM D5055 (ASTM International 2021) standards and undergoes performance evaluation under ASTM D7247 (ASTM International 2017). Although the I-joists themselves are not rated for specific fire durations, their performance under high temperatures is considered during fire-rating assessments of complete assemblies.

To further investigate the effect of elevated temperatures on I-joist properties, a statistical analysis was conducted to assess whether significant differences exist across various temperature levels. The data was subsequently modeled using a Sigmoidal non-linear model to capture the temperature-dependent behavior of I-joists. The Sigmoidal function, which

Table 2. Average compressive strength of I-joists at elevated temperatures.

		Exposure temperature (°C)								
Time	Stats	120	130	140	150	160	170	180	190	200
0 min	Mean (MPa)	1369	1268	1481	1209	1223	1254	1098	1021	739
	StaDev (MPa)	116	120	134	68	147	140	113	59	32
50 min	Mean (MPa)	1452	1477	1431	1269	1365	1215	1189	1103	852
	StaDev (MPa)	123	90	105	45	157	46	91	108	97
T-test p-values		0.30	0.01	0.53	0.13	0.18	0.58	0.20	0.18	0.06

Table 3. Average compressive MOE of I-joists at elevated temperatures.

		Exposure temperature (°C)								
Time	Stats	120	130	140	150	160	170	180	190	200
0 min	Mean (MPa)	4520	3284	4449	4101	3938	3977	3723	3435	2377
	StaDev (MPa)	494	1934	268	444	101	512	313	391	150
50 min	Mean (MPa)	4955	4735	4720	4173	4607	4076	3978	3839	2810
	StaDev (MPa)	448	264	563	465	420	253	641	479	534
T-test p-values		0.26	0.28	0.36	0.79	0.02	0.77	0.52	0.33	0.15

exhibits an "S-shaped" curve, is typically applied to processes that start slowly, accelerate, and then slow down again, such as growth and dose-response relationships (Weisstein 2007; Sánchez-Jiménez et al. 2022). This model effectively fits the thermal degradation behavior of materials under increasing temperatures.

Prior to the statistical analysis, the data for compressive strength and stiffness were evaluated for homogeneity of variance (Flinger test, $\alpha = 0.05$) and normality (Shapiro-Wilk test, $\alpha = 0.05$). Both tests confirmed that the data met the assumptions of equal variance ($p > 0.05$) and normal distribution ($p > 0.05$). Subsequently, analysis of variance (ANOVA, $\alpha = 0.05$) was performed to detect significant differences in properties across temperature groups. The ANOVA revealed a significant influence of temperature on both compressive strength and stiffness, with clear trends emerging at each exposure time.

To further examine pairwise differences between temperatures, Tukey's post-hoc tests were applied. The results were then modeled using the Sigmoidal function:

$$\sigma_c or\ E = \frac{a}{\left(1 + exp(b * (t - c)\right)} \quad [3]$$

Where σc represents the compressive strength (kPa), E is the modulus of elasticity (MPa), a is the maximum property value observed at the lowest tested temperature, t is temperature (°C), b controls the rate of degradation after the critical temperature, and c denotes the critical temperature at which rapid degradation begins. Both b and c were estimated by fitting the model to the data using the Levenberg-Marquardt nonlinear algorithm in R (RStudio Team 2023). Model parameters and R^2 values are summarized in Table 4.

To visualize these results, boxplots were created for both compressive strength and MOE, showing the results of the Tukey tests. Each box is annotated with letters indicating statistical differences between temperatures; boxes sharing the same letters do not differ significantly. A red dashed line represents the fitted Sigmoidal model, with the equation and model parameters displayed in the top right corner of each plot, as seen in Figure 2.

Table 4. Fitted parameters for compressive strength and MOE.

	Strength Parameters				MOE Parameters			
exposure	a	b	c	R^2	a	b	c	R^2
0 min.	1345	0.066	204	0.871	4520	0.053	206	0.924
50 min.	1477	0.043	210	0.927	4813	0.050	210	0.883

The TUKEY test results for compressive strength revealed a predictable decline with increasing temperature, with significant degradation becoming apparent at 180°C. Specifically, beyond 180°C, compressive strength at higher temperatures showed statistically significant differences compared to lower temperatures, indicating the onset of notable thermal degradation. Similarly, the MOE exhibited a decreasing trend, with significant differences observed at 200°C for both exposure times.

The Sigmoidal model provided further insights into the degradation pattern. It demonstrated a gradual decline in compressive strength and MOE at lower temperatures, followed by accelerated degradation at higher temperatures. The model's critical temperature parameter (c) indicated that significant degradation occurred around or slightly above 200°C. The model fit the data well, with R^2 values ranging from 0.81 to 0.90, validating its suitability for representing the non-linear degradation trends observed in materials exposed to high temperatures. This approach aligns with previous studies on the thermal degradation of materials but has not been widely applied to wood-based composites (Pan et al. 2024; Li and Kasal 2022).

Both the statistical analysis (Tukey test) and the Sigmoidal model indicated a significant reduction in I-joist mechanical properties—compressive strength and MOE—between 190°C and 210°C. Compressive failures were primarily attributed to buckling of the OSB web, with some failures involving prying of the LVL, which was likely caused by OSB flexure, followed by buckling, as seen in Figure 3. These findings are consistent with established degradation patterns of OSB, which begins to degrade between 175°C and 200°C (Sinha et al. 2011; Sugahara et al. 2022; Miyamoto and Sinha 2025). The thermal degradation of OSB can be attributed to both the decomposition of wood components, such as hemicellulose, and the breakdown of adhesives. Hemicellulose degradation typically begins at 170°C to 200°C, contributing to the observed loss in mechanical properties (Dietenberger and Hasburgh 2016; Sinha 2013). Additionally, the dramatic drop in mechanical properties at 200°C may be linked to the degradation of the polymeric methylene diphenyl diisocyanate (PMDI) adhesive used in OSB, which also begins to degrade around 200°C (Desai and O'Dell 1989; Yang et al. 1986).

To assess whether the Sigmoidal model would also be effective at lower temperatures, it was fitted to both the elevated temperature data and manufacturer-supplied compressive

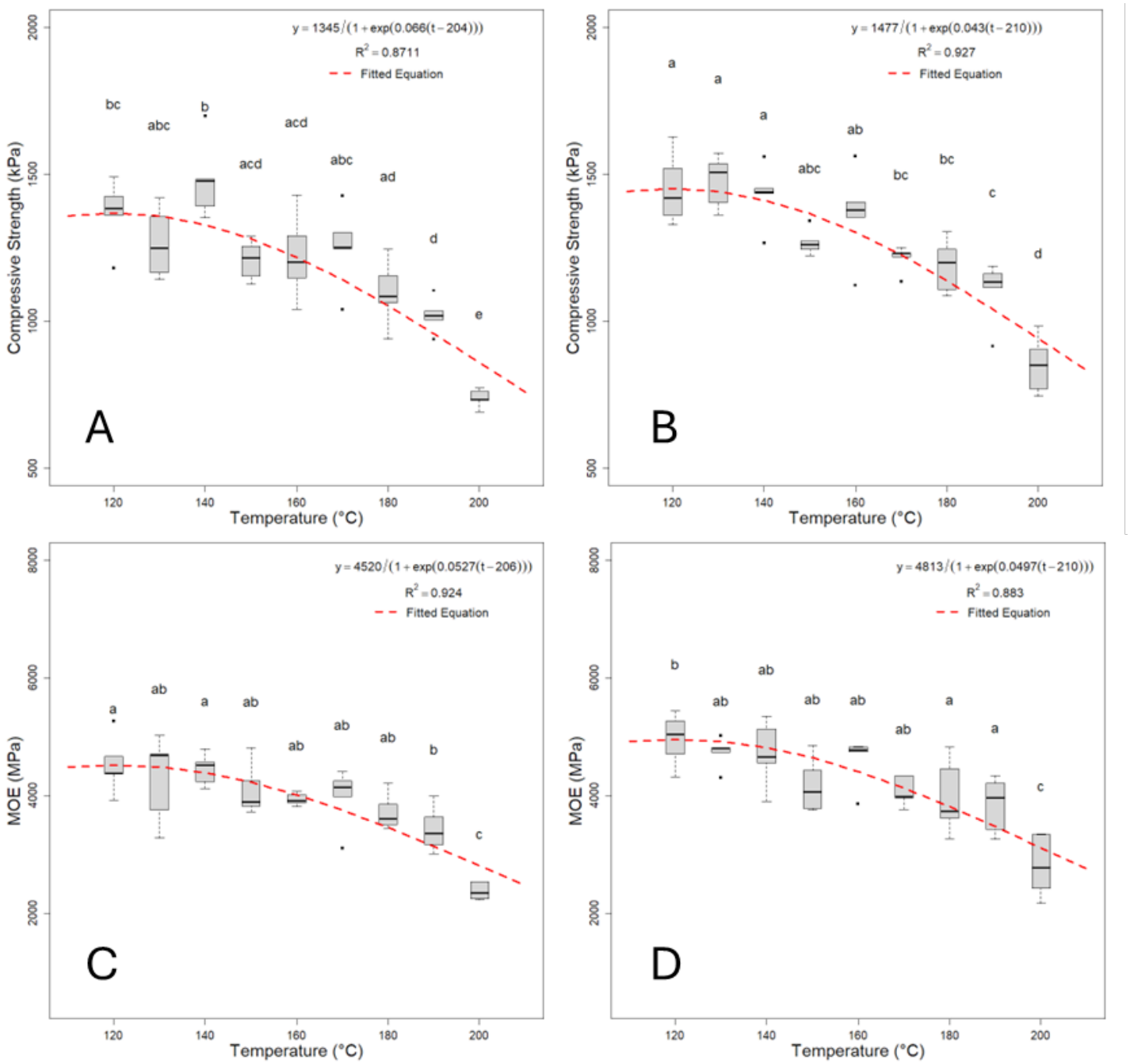

Figure 2. TUKEY test results for compressive strength at 0 min. (A) and 50 min (B) exposure times, and MOE at 0 min. (C) and 50 min. (D) exposure times, with the fitted Sigmoidal function model at both exposure times.

strength and MOE data for ambient conditions. This broader fitting provided a more comprehensive understanding of I-joist performance across a wide temperature range. The extended model results are shown in Figure 4.

The fitted parameters for the Sigmoidal model are shown in the top right corner of the graphs in Figure 4. The model demonstrated a good fit to the data, with R^2 values of 0.935 for compressive strength and 0.9147 for MOE. The shape of the curve is consistent with expectations, as thermal degradation is anticipated to commence at temperatures above 80°C and gradually progress, with accelerated degradation occurring at higher temperatures, such as 180°C to 200°C. While the model captures this general behavior, it may indicate the onset of thermal degradation at lower temperatures than expected. This model thus shows that it could be used as an empirical material model for thermal degradation.

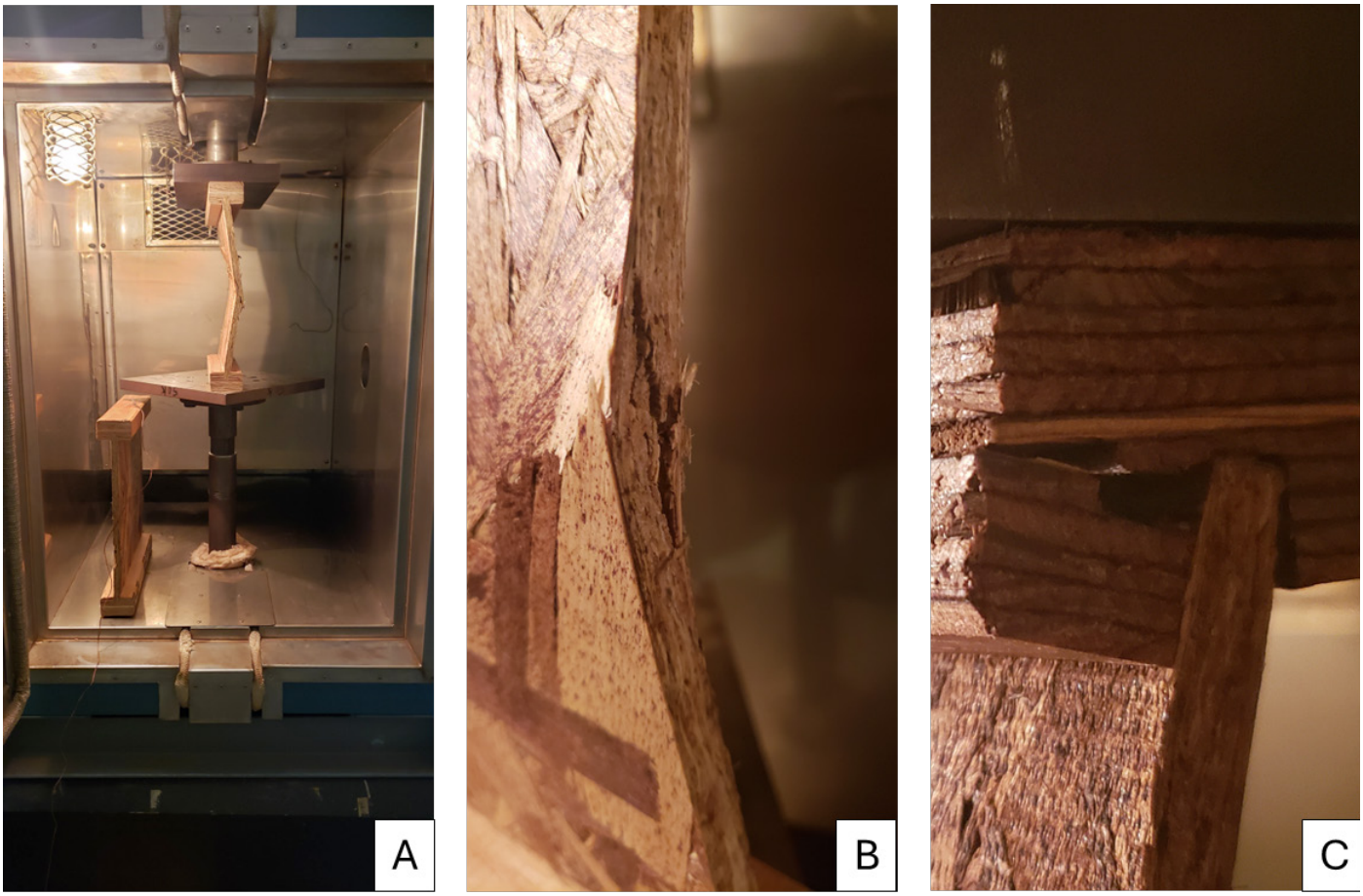

Figure 3. I-joist failure types. (A) Typical tested specimen failing in buckling; (B) OSB buckling failure; (C) LVL prying failure.

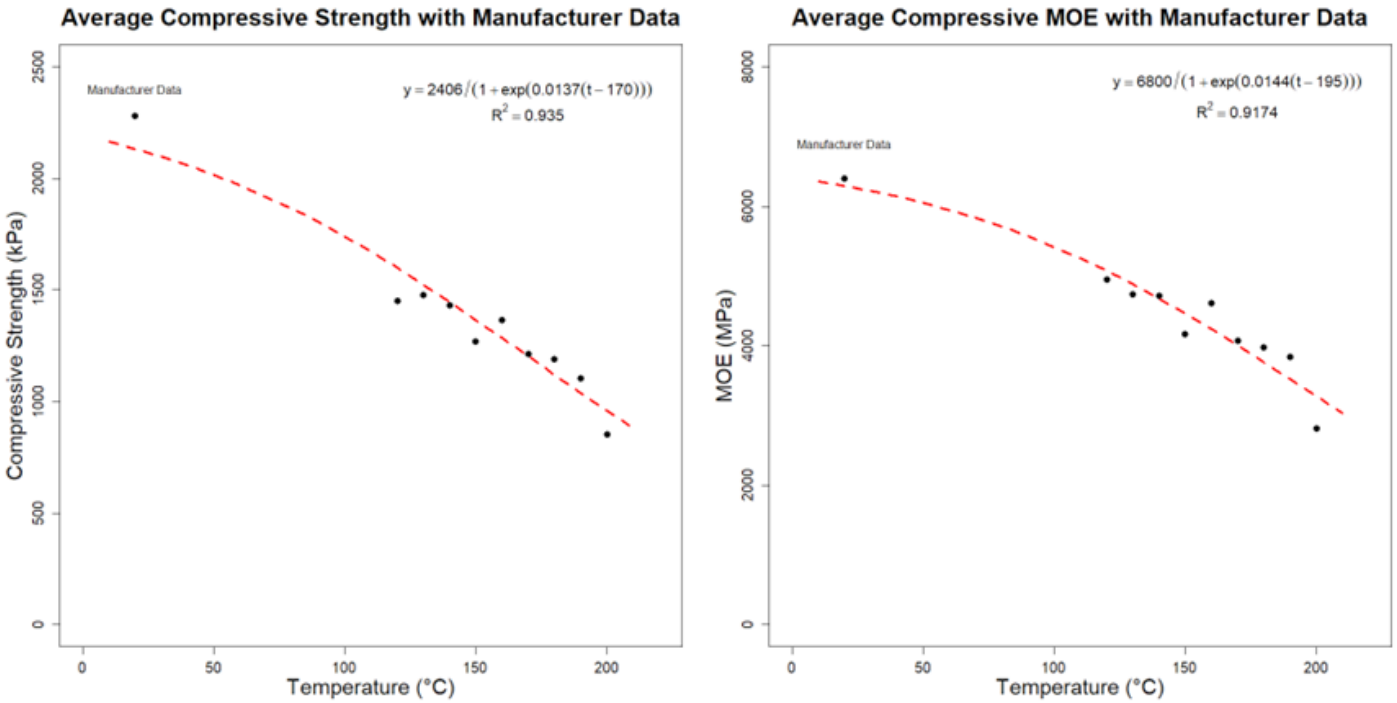

Figure 4. (A) Average compressive strength and (B) MOE at elevated temperatures and manufacturer data at room temperature with the fitted Sigmoidal function.

Conclusion

This study investigated the compressive properties of wooden I-joists under elevated temperatures. I-joists were tested at nine different temperatures, ranging from 120°C to 200°C, with two exposure times: one right when the specimen reached the target temperature and the other after 50 minutes of exposure. The tests followed a uniform vertical loading protocol in compression.

The results revealed that the OSB web was the primary failure mechanism, typically failing due to buckling. The two key properties evaluated were compressive strength and MOE. Both properties indicated significant thermal degradation beginning at approximately 190°C, with a drastic increase in degradation rates observed at 200°C. Interestingly, the comparison of the two exposure times showed no statistically significant differences. This suggests that temperature is the primary factor driving degradation, rather than the duration of exposure at high temperatures.

To further analyze the temperature-dependent behavior of the I-joists, a Sigmoidal model was fitted to the data. The model demonstrated a good fit, with R^2 values ranging from 0.81 to 0.90. The model also indicated that critical thermal degradation occurred primarily at temperatures of 200°C and above. An additional model fitting was performed, incorporating manufacturer data for I-joists tested at room temperature. This extended fit showed strong agreement, with R^2 values of 0.93 and 0.91 for compressive strength and MOE, respectively.

Future investigations into the compressive strength of I-joists at elevated temperatures should consider longer exposure durations to identify the critical time points at which compressive properties begin to degrade, as the two exposure times used in this study did not show significant differences. Additionally, testing at temperatures beyond 200°C, such as 220°C, would help validate the occurrence of thermal degradation at higher temperatures and could further refine the Sigmoidal model. Moreover, the effects of sustained constant loading on I-joists at elevated temperatures over extended exposure periods, such as 2 hours, should be explored to gain a deeper understanding of the long-term thermal behavior of these materials.

Acknowledgements

The authors would like to acknowledge the support of the Wood-Based Composites Center and the NSF INTERN program for funding this project.

References

APA – The Engineered Wood Association (2007) Wood I-joist floors, firefighters, and fire. APA – The Engineered Wood Association. Retrieved from https://www.apawood.org/Data/Sites/1/documents/fireprotection/fire-protection-requirements-for-IJ.pdf

APA – The Engineered Wood Association (2024a) PR-S259: Fire-rated assemblies for RFPI joists. Retrieved from https://www.apawood.org/download_pdf.ashx?pubid=80c89e03-9bb3-4c1c-bbfe-1f7496459874&bp=1

APA – The Engineered Wood Association (2024b) Performance Rated I-Joists Design and Construction Guide. https://www.apawood.org

ASTM International (2020) ASTM E119-20: Standard test methods for fire tests of building construction and materials. American Society for Testing and Materials, West Conshohocken, PA. USA. https://store.astm.org/standards/e119

ASTM International (2014) ASTM D7672-14: Standard specification for evaluating structural capacities of rim board products and assemblies. American Society for Testing and Materials, West Conshohocken, PA. USA. https://webstore.ansi.org/standards/astm/astmd767214

ASTM International (2021) ASTM D5055-21: Standard specification for establishing and monitoring structural capacities of prefabricated wood I-joists. American Society for Testing and Materials, West Conshohocken, PA. USA. https://store.astm.org/d5055-19e01.html

ASTM International (2017) ASTM D7247-17: Standard Test Method for Evaluating the Shear Strength of Adhesive Bonds in Laminated Wood Products at Elevated Temperatures. American Society for Testing and Materials, West Conshohocken, PA. https://store.astm.org/d7247-17.html

Desai HP, O'Dell JL (1989) Thermal stability and combustion characteristics of isocyanates in fire-retardant applications. Fire Mater 14(2):65–72.

Dietenberger MA, Hasburgh LE (2016) Wood Products: Thermal Degradation and Fire. In Reference Module in Materials Science and Materials Engineering (p. B9780128035818033385). Elsevier. https://doi.org/10.1016/B978-0-12-803581-8.03338-5

Grandmont J-F, Cloutier A, Gendron G, Desjardins R (2010) Effect of density on the properties of oriented strandboard web stock used in wood I-joists. For Prod J 60(7–8):592–598. https://doi.org/10.13073/0015-7473-60.7.592

ICC - International Code Council. (2024). ICC-ES Evaluation Report ESR-1336: Wood I-Joists (pp. 1–10). ICC Evaluation Service. https://cdn-v2.icc-es.org/wp-content/uploads/report-directory/ESR-1336.pdf

King DT, Sinha A, Morrell JJ (2014) Effects of outdoor exposure on properties of I-joists. Wood Fiber Sci 46(3):394–400. https://wfs.swst.org/index.php/wfs/article/view/264

Li J, Kasal B (2022) Effects of Thermal Aging on the Adhesion Forces of Biopolymers of Wood Cell Walls. Biomacromolecules 23(4):1601–1609. https://doi.org/10.1021/acs.biomac.1c01397

Miyamoto BT, Sinha A (2025) Time-temperature effects on early-stage primary thermal creep of plywood and oriented strand board (OSB) at elevated temperatures. Wood Fib Sci 57(1):15-26. https://doi.org/10.22382/wfs-2025-02

Morrissey GC, Dinehart DW, Dunn WG (2009) Wood I-Joists with Excessive Web Openings: An Experimental and Analytical Investigation. J Struct Eng 135(6):655–665. https://doi.org/10.1061/(ASCE)ST.1943-541X.0000013

NAHB - National Association of Home Builders (2023) Restrictions and bans on wood trusses and I-joists (Policy Resolution No. 2023/6-7). https://www.nahb.org/-/media/NAHB/advocacy/docs/policy-resolutions/construction-and-codes/2023-6-no-7-restrictions-and-bans-on-wood-trusses-and-i-joists.pdf?rev=675e5f2531264a8980b1f79b9dfd637b

NAHB - National Association of Home Builders (1999) Restrictions and bans on wood trusses and I-joists (Policy Resolution No. 1999/5-14). https://www.nahb.org/-/media/NAHB/advocacy/docs/policy-resolutions/construction-and-codes/1999-5-no14-restrictions-and-bans-on-wood-trusses-i-joists.pdf

Pan B, Shen F, Sampathkumar SR, Münstermann S (2024) Modeling strain hardening of metallic materials with Sigmoidal function considering temperature and strain rate effects. Materials 17(16):3950. https://doi.org/10.3390/ma17163950

RStudio Team (2023) RStudio: Integrated Development for R. RStudio, PBC. Retrieved from https://www.rstudio.com/

Sánchez-Jiménez PE, Perejón A, Arcenegui-Troya J, Pérez-Maqueda LA (2022) Predictions of polymer thermal degradation: Relevance of selecting the proper kinetic model. J Therm Anal Calorim 147(3):2335–2341. https://doi.org/10.1007/s10973-021-10649-x

Siimer K, Kaljuvee T, Pehk T, Lasn I (2010) Thermal behaviour of melamine-modified urea–formaldehyde resins. J Therm Anal Calorim 99(3):755–762. https://doi.org/10.1007/s10973-009-0617-z

Sinha A (2013) Thermal degradation modeling of flexural strength of wood after exposure to elevated temperatures. Wood Mater Sci Eng 8(2):111–118. https://doi.org/10.1080/17480272.2012.753950

Sinha A, Gupta R, Nairn JA (2011). Thermal degradation of bending properties of structural wood and wood-based composites. Holzforschung 65(2):221–229. https://doi.org/10.1515/hf.2011.001

Smulski S, ed. (1997) Engineered wood products: A guide for specifiers, designers & users. PFS Research Foundation. ISBN: 9780965673600

Sugahara E, Dias A, Arroyo F, Christoforo A, Costa ML, Botelho EC, Dias AMPG, Campos C (2022) Study of the influence of heat treatment on OSB panels produced with Eucalyptus wood in different layer compositions. Forests 13(12):2083. https://doi.org/10.3390/f13122083

Sultan MA, Seguin YP, Leroux P (2007) Fire resistance of wood-frame assemblies. Fire Technol 45(2):113–128. https://doi.org/10.1007/s10694-007-0038-0

Forest Products Laboratory (2010) Wood handbook: Wood as an engineering material. General Technical Report FPL-GTR-190. Madison, WI: U.S. Department of Agriculture, Forest Service, Forest Products Laboratory. https://www.fpl.fs.usda.gov/documnts/fplgtr/fpl_gtr190.pdfFisette, P (2000). The evolution of engineered wood I-joists. Building and Construction Technology. Retrieved from https://www.umass.edu/bct/publications/articles/the-evolution-of-engineered-wood-i-joists/

Way D, Sinha A, Kamke FA (2018) Laboratory and Outdoor Weathering of Wood-Composite I-Joists. J Mater Civ Eng 30(7):04018148. https://doi.org/10.1061/(ASCE)MT.1943-5533.0002327

Weisstein EW (2007) Sigmoid function. In MathWorld – A Wolfram Web Resource. Retrieved from https://mathworld.wolfram.com/SigmoidFunction.html

Yang WP, Macosko CW, Wellinghoff ST (1986) Thermal degradation of urethanes based on 4,4′-diphenylmethane diisocyanate and 1,4-butanediol (MDI/BDO). Polymer 27(8):1235–1240. https://doi.org/10.1016/0032-3861(86)90012-1

Yeh B, Herzog B (2018) Effect of holes on the structural capacities of laminated veneer lumber. In Proceedings of the 2018 World Conference on Timber Engineering. Seoul, Republic of Korea: APA – The Engineered Wood Association. Retrieved from https://www.apawood.org/Data/Sites/1/documents/technicalresearch/MAT-012-04_Effect-of-Holes-on-the-Structural-Capacities-of-LVL_FullPaper.pdf